

# Ion Thruster Plume Plasma Interactions in the Solar Wind

Joseph Wang

Jet Propulsion Laboratory, California Institute of Technology, Pasadena

## 1. Introduction

Ion propulsion will be used for the first time on an interplanetary spacecraft, Deep Space One (DS1), scheduled for launch in July 1998. A primary objective of New Millennium DS 1 is to flight validate solar electric propulsion (SEP) for interplanetary missions. The cruise phase of the mission will characterize the life and performance of a 30 cm xenon ion thruster and determine how its operation may affect spacecraft payloads and critical subsystems...

Effects introduced by the operation of the ion thruster have long raised both technology and science concerns. The technology concerns include plume backflow contamination and spacecraft interactions with the induced plasma environment. Backflow contamination can lead to effluent deposition that can affect thermal control surfaces, optical sensors, solar arrays, science instrumentation, and communications. The induced plasma environment will modify spacecraft charging characteristics, and can lead to plasma interactions with the solar array. The science concerns relate to plasma measurements. The plume will modify the properties of the solar wind flowing around the spacecraft and may contaminate measurements of the ambient plasma and magnetic fields. As ion thrusters are designed to operate for long periods of time, these effects need to be carefully assessed.

The interactions induced by ion thruster plumes have been studied for some time. Due to the complexity of the problem, the difficulty of matching space conditions in a laboratory, and the lack of opportunities to flight test ion thrusters, computer particle simulations have recently become the best means to study this problem. *Samanta Roy et al.*[1996a,1996b] used hybrid PIC simulations to model the far-downstream region and study charge exchange ion backflow. *Wang and Brophy*[1995] developed full particle and hybrid PIC-MCC models of single and multiple thruster plumes and studied the effects of ambient environment on plasma plumes. *Wang et al.*[1996] have carried out 3-D simulations of ion thruster plume environments using parameters similar to those of the NSTAR (NASA Solar-Electric Propul-

sion Technology Application Readiness) thruster to be used on DS1. All studies on this subject so far have concentrated on charge-exchange ion interactions near the spacecraft. There have been no studies concerning other aspects of plume interactions, such as ion thruster operation in the solar wind environment and plume-solar wind interactions.

For an interplanetary spacecraft such as the DS-1, the ion thruster operates in the solar wind, which is a tenuous, relatively hot plasma with a high flow speed and a frozen-in magnetic field. It is instructive to first review theoretical studies of solar wind interactions with newborn ions related to comets and collisionless shocks. Generally speaking there are three mechanisms by which newborn ions may interact with the solar wind plasma and magnetic field. The first is particle/particle Coulomb collisions which is relatively weak due to the low density of the solar wind. The second process is cyclotron pickup, in which the motional electric field of the solar wind accelerates the newborn ion which then gyrates around a magnetic field line. The third mechanism is scattering of the ions by wave/particle interactions. The consequences of the collisionless second and third mechanism are studied in numerous papers for homogeneous plasmas. For instance, *Wu and Davidson*[1972] are among the first to point out that the newly ionized particles in the solar wind can result in collective instabilities that generate large-amplitude electromagnetic waves. *Gary et al.* [1984,1986] presented linear theories and 1-dimensional simulations of electromagnetic instabilities driven by a cool ion beam parallel or anti-parallel to the solar wind magnetic field. *Omidi and Winske*[1987] performed hybrid simulations on the kinetic processes associated with solar wind mass loading due to pickup of cometary ions and the formation of cometary bow shocks. A review of electromagnetic ion/ion instabilities in space plasmas is found in [*Gary*,1991].

Solar wind/ion couplings have never been examined within the context of ion propulsion. In principle, kinetic couplings between the solar wind and newborn ions could also occur to an ion thruster plume in the solar wind. However, since the properties of an ion

thruster plume are very different from those of cometary ions or cosmic ray particles (for instance, the density of the plume is much higher than that of the solar wind), it is not clear whether any plume-solar wind interactions could occur, and if they can, what the consequences would be.

In this paper we study ion thruster plume interactions in the solar wind. We first briefly discuss the properties of the plasmas emitted from the NSTAR ion thruster and the resulting near-field plume interactions in section 2. This establishes the properties of the ion thruster plume in the absence of the ambient environment. In section 3, we study plume solar wind interactions. Our emphasis here is to investigate whether any plume-solar wind coupling may occur via collisionless mechanisms. Hence, we shall consider interactions far away from the thruster exit where the plume has become sufficiently rarefied so that the solar wind can penetrate into the plume. Section 4 contains a summary and conclusions.

## 2. Ion Thruster Plume

### The Ion Thruster Plasma

In ion thrusters, propellant ions are accelerated electrostatically by a system of grids to form a high velocity beam; neutralizing electrons are emitted from the neutralizer in conjunction with the beam ions. Thus the ion thruster plume is composed of propellant efflux (including beam ions, neutralizing electrons, and neutrals that escape through the ion optics and from the neutralizer), nonpropellant efflux (material sputtered from thruster components and the neutralizer), and a low-energy plasma generated through charge-exchange collisions between energetic ions and the neutrals within the plume.

The 30 cm xenon NSTAR thruster to be used on DS1 has an input power range of 600 to 2500 W. Under typical operating conditions, the beam current is about 1.76 A; and the exit beam velocity is about  $3.5 \times 10^6$  cm/s (beam ion kinetic energy about 1 keV); Near the thruster exit, the temperature of beam ions is about 0.04 eV ( $\sim 500$  K), and the temperature of the neutralizing electrons is in the range of 1-5 eV. From these parameters, the average beam ion current at the thruster exit is  $J_{bi0} = I/\pi r_T^2 \simeq 24.9 A/m^2$  and the average beam ion density at the thruster exit  $n_{b0} = J_{bi0}/ev_{bi} \simeq 4.4 \times 10^9 cm^{-3}$ . The propellant ions form a divergent beam with a divergence half angle about 15 to 20° due to the curvature of the thruster exit surface. The radial beam current density profile may be assumed to follow a Gaussian distribution, although the actual distribution may be more peaked at the center.

The propellant that remains unionized flows out of the thruster exit in free molecular flow at thermal speeds corresponding to the thruster wall temperature ( $\sim 500$  K). The density of the neutral plume near the thruster exit is about  $10^{12} cm^{-3}$  and remains quasi-steady due to the low charge-exchange collision rate. For  $v_{bi} \simeq 3.5 \times 10^6$  m/s, we find that the charge-exchange collision cross section  $\sigma_{cex} \simeq 3.5 \times 10^{-15} cm^2$ . Hence, at the thruster exit, we find the charge-exchange ion production rate  $\frac{dn_{cex0}}{dt} \simeq 2.4 \times 10^{13} cm^{-3}s^{-1}$ . In addition to these propellant and charge-exchange ions a very small amount of neutrals may also undergo photoionization or charge-exchange ionization in the solar wind.

### Near-Spacecraft Plume Environment

We first review ion thruster plume interactions near the spacecraft. As the solar wind density is about  $1 cm^{-3}$  it is appropriate to neglect the solar wind plasma as a first approximation. Under the solar wind magnetic field, the gyroradius for the beam ions and the charge exchange ions is much larger than the size of the spacecraft. Hence, the solar wind magnetic field can also be neglected for the near-field region. Thus, the interaction is electrostatic.

During normal ion thruster operation, electron emission keeps the exhaust plume quasineutral and prevents the spacecraft from charging up significantly. Typically the spacecraft potential  $\Phi_{s/c}$  is much lower than that of the beam ion kinetic energy,  $|e\Phi_{s/c}| \ll KE_{bi0}$ . In the absence of an external electromagnetic field, the beam ions follow nearly line-of-sight trajectories because the electric field within the plume is too small to perturb their motion. Hence, the core region of the ion beam will keep its coherent structure. The electrons are much more mobile than ions, so the center of the plume has a positive potential. This potential causes the slowly moving charge-exchange ions to move transversely out of the plume.

Wang *et al.* [1995,1996] have developed a fully three-dimensional hybrid particle-in-cell Monte Carlo collision model of the near-field plume environment. In this model, the ions are represented by individual superparticles and the electrons are assumed to have a fluid response in which the density is given by the Boltzmann distribution. A typical simulation setup is shown in Fig.1a. The spacecraft is modeled as a 3-dimensional box structure with a conducting surface and a surface potential  $\Phi_w$  relative to the ambient. At each time step, the propellant ions are injected into the simulation domain from the thruster exit to form a beam with a Gaussian density distribution in the radial direction and a divergent half angle of 15°. The neutral plume is treated as a steady state background produced by a free

“molecular flow. A Monte Carlo representation of particle collisions is utilized to model the charge-exchange collision between the beam ions and the neutral background. The charge-exchange ions are generated according to

$$\frac{dn_{cex}}{dt} = n_{bi}n_n v_{bi} \sigma_{cex}(v_{bi}) \quad (1)$$

based on the beam ion and neutral density profile. The trajectory of each charged particle is integrated from

$$\frac{dm\vec{V}}{dt} = \vec{F} = q(\vec{E} + \vec{V} \times \frac{\vec{B}}{c}), \quad \frac{d\vec{x}}{dt} = \vec{V} \quad (2)$$

using a standard leapfrog scheme, and the self-consistent electric field is obtained from the Poisson's equation

$$\nabla^2 \Phi = -4\pi\rho \quad (3)$$

Some typical simulation results are shown in Fig. 2. For this simulation, the spacecraft is taken to be a cubic box with dimension  $1m \times 1m \times 1m$ . The spacecraft is located at  $2 \leq x \leq 16$ ,  $15 \leq y \leq 29$ , and  $15 \leq z \leq 29$ . The thruster exit center is located at  $x = 18$ ,  $y = 22$ , and  $z = 22$ . The thrust direction is in the  $x$  direction. The grid resolution is taken to be  $dell \simeq 5.2cm$ . The spacecraft potential is taken to be  $\Phi_s/c/T_e \simeq -3$ . Fig.2 shows the contours of potential and the total ion density and the vectors of the charge-exchange ion current density on a  $xy$  plane cutting through the spacecraft and thruster center. We find that the outflow of the charge-exchange ions forms a wing-shaped structure. Once outside the plume, the charge-exchange ions come under the influence of the potential of the spacecraft sheath. As the spacecraft potential is typically negative, these ions will therefore be drawn back to the spacecraft.

### 3. Far-Field Plume-Solar Wind Interactions

#### The Solar Wind Plasma

We next consider the ion thruster plume in the solar wind plasma. The solar wind is a tenuous, relatively hot plasma which flows radially outward from the sun. Since the magnetic field is approximately “frozen” in the conducting solar wind, the solar magnetic field is convected out into space by the solar wind. The expansion of the solar wind plasma across the interplanetary magnetic field also induces a motional electric field in the reference frame at rest with respect to the Sun,  $\vec{E}_o = -\vec{v}_{sw} \times \vec{B}_o$ . In the reference frame of the solar wind,  $\vec{E} \simeq O$ . The solar wind parameters may undergo substantial variation, but typical values are: solar wind density  $n_{sw} \sim 1 cm^{-3}$ , solar wind flow speed  $v_{sw} \sim 350 km/s$ , solar wind ion temperature  $T_i \sim 10 eV$ , and

solar wind magnetic field magnitude  $B_o \sim 10 nT$ . The angle between the solar wind flow velocity  $\vec{v}_{sw}$  and the interplanetary magnetic field  $\vec{B}_o$ ,  $\alpha$ , can vary from  $0^\circ$  to  $90^\circ$  and is a crucial parameter in much of the physics involved.

#### Formulation and Approach

The global scale plume-solar wind interaction is illustrated in Fig.1b. The plume-solar wind interaction has very different characteristics from the near-field plume-spacecraft interaction. While the plume-spacecraft interaction is electrostatic in nature, the couplings between the plume ion and the solar wind is electromagnetic in nature. While the plume-spacecraft interaction occurs in the vicinity of the spacecraft, the plume-solar interaction would occur at a global scale. This is because, if any solar wind/ion coupling could occur, the characteristic electromagnetic wave length would be much larger than the spacecraft size.

Our approach is based on electromagnetic hybrid particle simulation [ Winske and Omid,1993]. Since the interactions only concern the ion dynamics, the basic assumptions in our approach are a) the electrons are a massless fluid  $m_e = O$  while the ions are treated as test particles, and b) the displacement current  $\frac{\partial \vec{E}}{\partial t}$  can be neglected in Ampere's law (for low frequency waves). Since we are concerned with a quasineutral plasma in a global region, quasineutrality is assumed. Therefore, the governing equations are

1) Quasineutrality:

$$n_e = n_i \quad (4)$$

2) Maxwell's equations in the low frequency approximation:

$$\nabla \times \vec{B} = \frac{4\pi}{c} \vec{J} \quad (5)$$

$$\nabla \times \vec{E} = \frac{\partial \vec{B}}{\partial t} - \frac{1}{c} \quad (6)$$

$$\nabla \cdot \vec{B} = 0 \quad (7)$$

3) The electron fluid equation in the limit of  $m_e = O$ :

$$\frac{\partial n_e m_e \vec{V}_e}{\partial t} = 0 = -en_e(\vec{E} + \vec{V} \times \frac{B}{c}) - \nabla \cdot \mathbf{P}_e + en_e \mathbf{R} \cdot \vec{J} \quad (8)$$

where the electron pressure tensor is given by:

$$\mathbf{P}_e = n_e T_e \mathbf{I} \quad (9)$$

and the resistivity tensor  $\mathbf{R} = \eta \mathbf{I}$  describes short wavelength, high frequency wave-particle interactions not explicitly included in the hybrid model; and

4) Dynamic equation for individual ion particles

$$m_i \frac{d\vec{v}_i}{dt} = \vec{F} = q(\vec{E} + \vec{v}_i \times \frac{\vec{B}}{c}) - q\eta \vec{J}, \quad \frac{d\vec{x}_i}{dt} = \vec{v}_i \quad (10)$$

In this paper, we only consider the far-field region where the plume has become sufficiently rarefied so that the solar wind can penetrate into the plume. For convenience, we choose a reference frame moving with the solar wind. Hence the solar wind sees a plume moving with a relative velocity  $-\mathbf{v}_{sw} + \mathbf{v}_{plume}$ . As  $\mathbf{v}_{sw}$  is much larger than the beam ion velocity, the relative drift velocity between the solar wind and the plume is dominated by the solar wind flow speed. Hence, we do not need to distinguish between the beam ions and the charge-exchange ions. Since our emphasis here is on the consequences of the collisionless process, we shall consider a  $2\frac{1}{2}$ -dimensional (2 spatial components, three velocity and field components), homogeneous model shown in Fig.1b. We take the relative velocity  $\mathbf{v}_{dx} = -\mathbf{v}_{sw} + \mathbf{v}_{plume}$  along the x direction, and the angle between x and the solar wind magnetic field to be  $\alpha$ . Initially, the solar wind protons follow a Maxwellian distribution with a temperature of 10 eV and the plume ions follow a drifting Maxwellian distribution centered around  $\mathbf{v}_{dx}$  with a temperature of 0.04 eV.

## Results and Discussions

In the simulations presented here we consider two flow conditions, the parallel flow ( $\alpha = 0^\circ$ ) and the perpendicular flow ( $\alpha = 90^\circ$ ) conditions. We take the plume to solar wind density ratio to be  $n_X/n_{sw} \sim 100$ .

The simulation results are presented in Fig.3 through Fig.6. Due to computational limitations, an artificial proton mass of  $m_p/m_X = 16-1$  is used. This compresses the relative plume ion and solar wind proton gyroperiods but does not affect the qualitative picture of the physics. In the solar wind reference frame, the relative plume velocity normalized by the Alfvén speed for the plume ions,  $v_{AX} = B_o / \sqrt{4\pi n_X m_X}$ , is  $v_{dx}/v_{AX} \simeq 63.2$ .

The velocity distributions for the plume ions and the solar wind protons for the  $\alpha = 0^\circ$  case are shown in Fig. 3. The distribution functions are shown for  $t\Omega_X = 0, 8, 16, 24, \text{ and } 48$ , where  $\Omega_X$  is the gyro frequency of the plume ions under the solar wind magnetic field. At the early stage of the interaction ( $t\Omega_X \leq 8$ ), the velocity distributions for the plume ion show little change. However, the distribution functions for the solar wind protons have changed from an isotropic Maxwellian distribution to a drifting Maxwellian with a drifting speed about  $0.16v_{dX}$  along the x direction. This indicates that the solar wind protons are partially “picked up” by the plume. At the later stage of the interaction ( $t\Omega_X > 16$ ), the plume ions start to lose their drifting speed and thermalize. At  $t\Omega_X \geq 48$ , we find that the plume ions have completely thermalized into a isotropic distribution. In other words, in the reference frame of the sun,

the plume ions are swept away by the solar wind as a warm cloud. Hence, the plume has lost its original properties

The velocity distribution functions for the  $\alpha = 90^\circ$  case are shown in Fig. 5. The plume ions behave similarly to that for the  $\alpha = 0^\circ$  case, although the thermalization starts a little later. The solar wind protons settle to a drifting distribution with a drifting speed about  $0.19v_{dX}$  during the first stage. During the second stage, the relaxation process is slower in the direction parallel to  $\mathbf{B}_o$ .

To understand these results, we analyze the time history of the plume ion energies associated with the three velocity components and the magnetic wave energy density in the system  $((\delta B/B_o)^2)$  (Figs. 4 and 6). For the  $\alpha = 0^\circ$  case, we find that the magnetic wave energy starts to grow exponentially at  $t\Omega_X \sim 15$ , indicating an electromagnetic instability is excited. As the instability grows, wave-particle interactions drive the system toward isotropy and reduces the amount of free energy available for wave growth. Hence, the growth of wave energy is accompanied by a decrease of  $v_x$  and increases in  $v_y$  and  $v_z$ . The wave energy saturates at an almost constant level at  $t\Omega_X \simeq 40$ . The fact that  $(\delta B/B_o)^2 \gg 1$  after instability excitation suggests that the wave-particle interaction is strongly non-linear. For the  $\alpha = 90^\circ$  case, the time histories have similar characteristics. However, the magnetic field fluctuations is only about 40% of that for  $\alpha = 0^\circ$ . This indicates that the instability is weaker in the  $\alpha = 90^\circ$  case.

The physics of the collisionless plume ion-solar wind coupling can be summarized as follows. Under the perpendicular flow condition,  $\alpha \sim 90^\circ$ , cyclotron pickup leads to a ring-shaped newborn ion velocity distribution. Under the parallel flow condition,  $\alpha \sim 0^\circ$ , there are no magnetic forces on the newborn ions and the resulting distribution is a beam moving along the background magnetic field relative to the solar wind distribution. If  $\alpha$  has an intermediate value, the newborn ions assume a ring-beam distribution. These non-Maxwellian distributions represent a strong source of free energy relative to the solar wind ion velocity distribution, and can excite a variety of instabilities which lead to enhanced fluctuations which, in turn, scatter the plume ions toward isotropization [Gary, 1991].

## 4. Summary and Conclusions

We have developed a global analysis of ion thruster plume interactions for interplanetary spacecraft which includes a fully 3-dimensional electrostatic PIC-MCC model for near-field interactions and a  $2\frac{1}{2}$ -dimensional

electromagnetic hybrid PIC model for far-field plume-solar wind couplings. We show that different physical process dominates in different plume regions. In the near-field region of the spacecraft, the interaction is driven by the low energy charge-exchange ions responding to the electrostatic potential. The presence of the solar wind environment may induce complex plume-solar wind interactions. In the vicinity of the thruster, since the thruster plume will dominate the spacecraft environment due to their much higher density, the main effect of the plume is simply to modify the solar wind as it flows past the plume region. However, far away from the thruster where the plume density has decreased to a level that the solar wind plasma and fields can penetrate the plume, we find that the plume ions may couple with the solar wind through collective plasma effects. This is because both the low energy charge-exchange ions and the energetic beam ions constitute a free energy source, which may drive one of several electromagnetic instabilities. The instabilities can generate enhanced magnetic field fluctuations, leading to significant particle scattering. This wave particle scattering will modify the properties of both the solar wind and the plume. Due to the large amount of free energies carried by the plume, the wave-particle interactions are highly non-linear, and can scatter the beam ions and charge-exchange ions into an isotropic distribution in the solar wind reference frame. This raises the possibility that far-field interactions may affect the plasma environment in the vicinity of the spacecraft. The scenario for maximum plume-solar wind coupling would be for the ion thruster to thrust in the direction anti-parallel to the local solar wind flow direction.

The far-field analysis presented in this paper only addresses the possibility and the mechanisms of solar wind-plume interactions but does not attempt to quantify the effects of far-field interactions on the near-field environment. We only considered interactions in the far-field and assumed that the solar wind has penetrated into the plume. The homogeneous model also does not address the effects of finite plume size which inhibits growth of the electromagnetic instabilities. These issues will be addressed in our future work, which will extend this study to 3-D hybrid electromagnetic simulations to resolve plume-solar wind coupling in a global interaction region.

### Acknowledgement

I would like to thank S. Peter Gary of Los Alamos National Lab and John Brophy, Dave Brinza, and Paulett Liewer of JPL for many useful discussions. This work was carried out by the Jet Propulsion Laboratory, California Institute of Technology under a contract with

NASA. Access to the Cray supercomputers used in this study was provided by funding from NASA Offices of Mission to Planet Earth, Aeronautics, and Space Science.

### References

- [1] S.P. Gary, C. Smith, M. Lee, M. Goldstein, D. Forslund, Electromagnetic ion beam instabilities, *Phys. Fluids*, 28, 1984, pp438
- [2] S.P. Gary, C. Madland, D. Schriver, and D. Winske, Computer simulations of electromagnetic cool ion beam instabilities, *J. Geophys. Res.*, 91(A4), 1986, pp4188.
- [3] S.P. Gary, Electromagnetic ion/ion instabilities and their consequences in space plasmas: a review, *Space Sci. Reviews*, 56, 1991, pp373.
- [4] Omid and Winske, A kinetic study of solar wind mass loading and cometary bow shocks *J. Geophys. Res.*, 92( A12), 1987, pp13409.
- [5] R. Samanta Roy, D. Hastings, and N. Gatsonis, Ion-thruster modeling for backflow contamination, *J. Spacecraft Rockets*, 33(4), 1996a, pp525.
- [6] R. Samanta Roy, D. Hastings, and N. Gatsonis, Numerical study of spacecraft contamination and interactions by ion-thruster effluents, *J. Spacecraft Rockets*, 33(4), 1996b, pp535.
- [7] J. Wang and J. Brophy, 3-D Monte-Carlo particle-in-cell simulations of ion thruster plasma interactions, *41,4A Pap. 95-2826*, 1995.
- [8] J. Wang, J. Brophy, and D. Binza, 3-D simulations of NSTAR ion thruster plasma environment, *AIAA Pap. 96-9202*, 1996.
- [9] D. Winske and N. Omid, Hybrid codes, methods and applications, in *Computer Space Plasma Physics: Simulation Techniques and Software*, edited by H. Matsumoto and Y. Omura, Tokyo, 1993.
- [10] C. Wu and R. Davidson, Electromagnetic instabilities produced by neutral-particle ionization in interplanetary Space, *J. Geophys. Res.*, 77(28), 1972, pp5399.

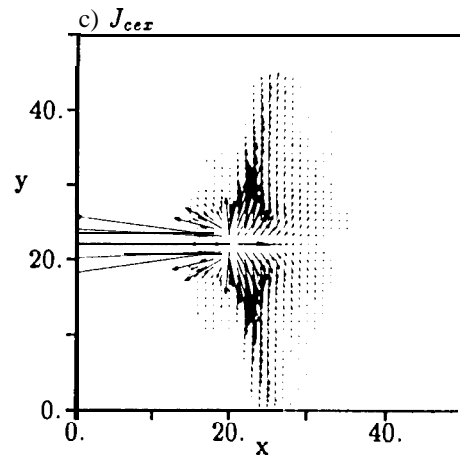
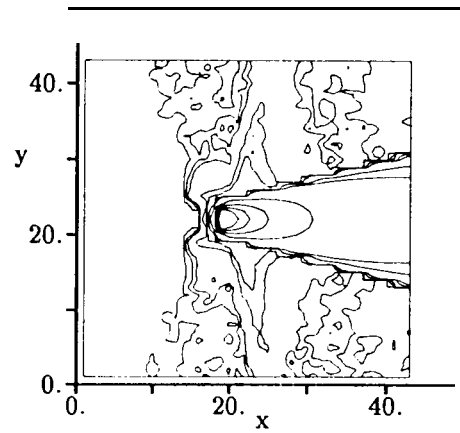
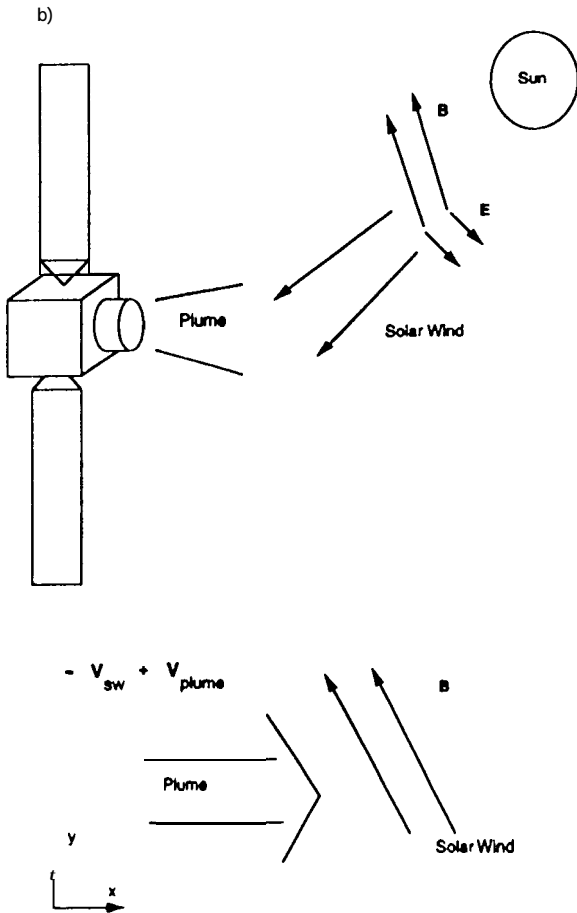
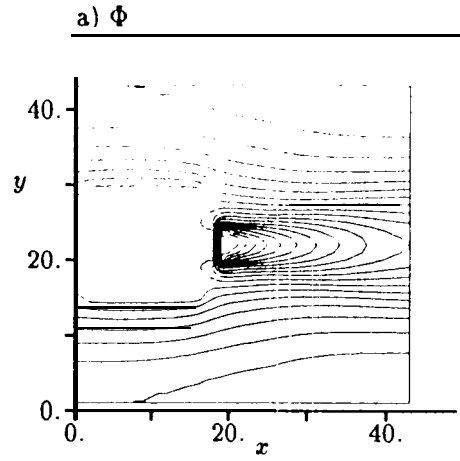
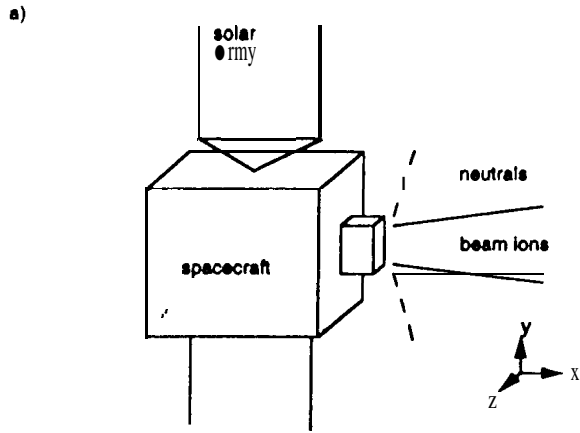
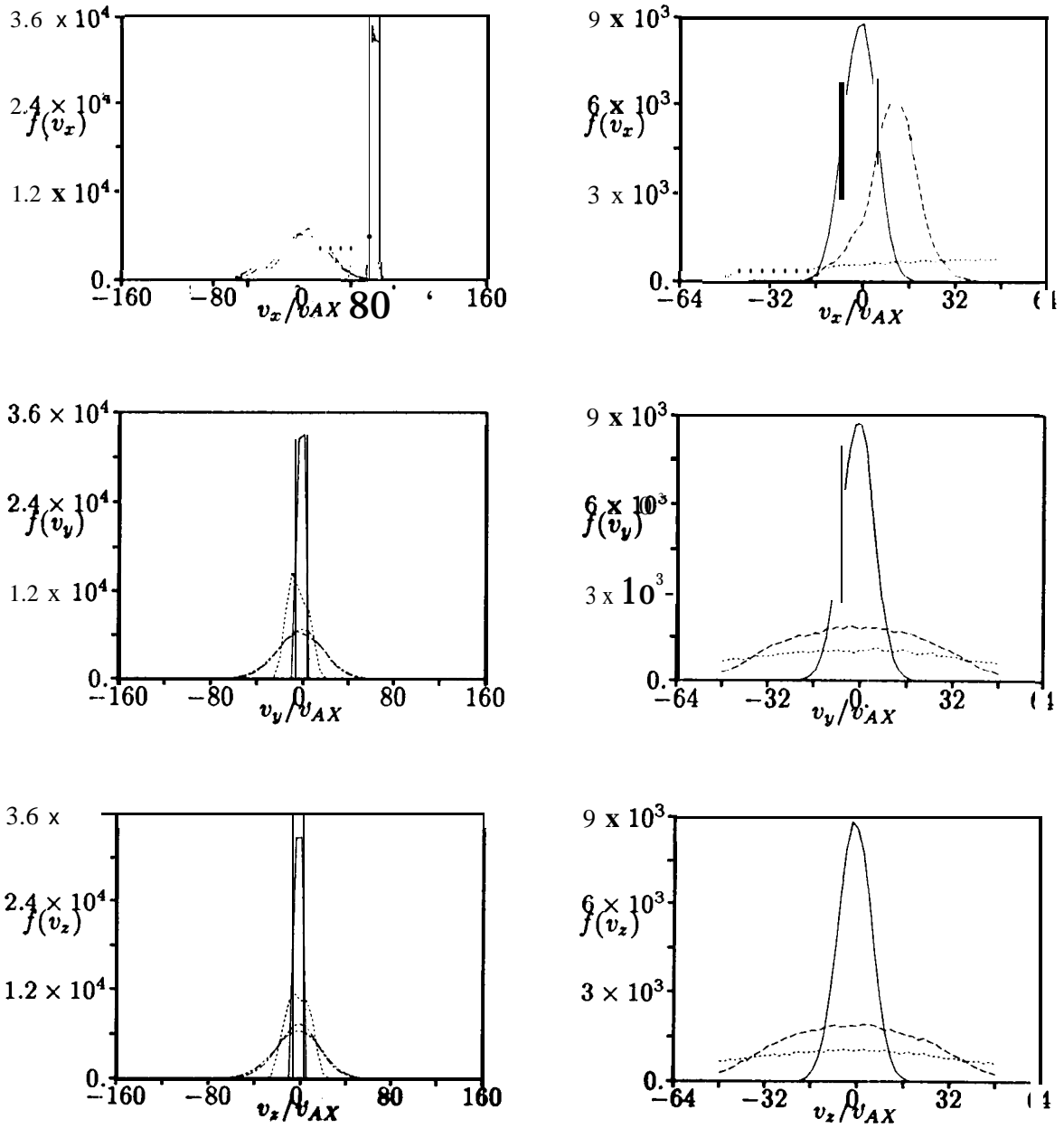
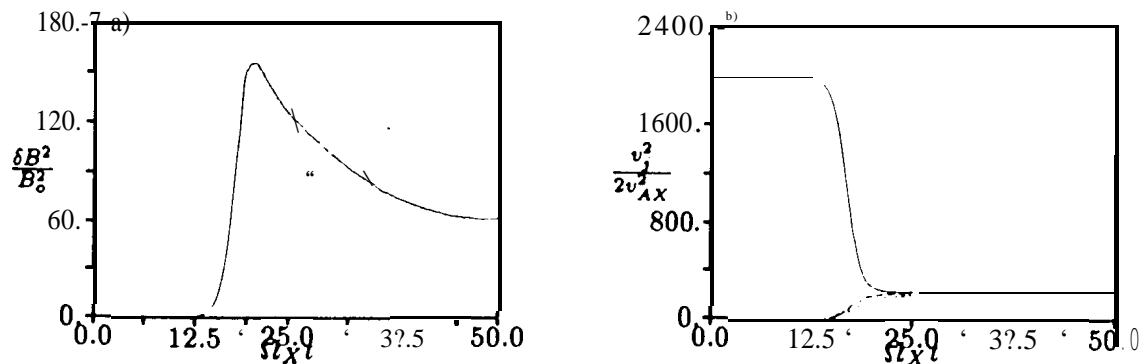


Figure 1: Model setup. a) Near-field interaction model. b) Far-field interaction model.

Figure 2: Plasma plume on a xy plane cutting through the center of thruster and spacecraft, a) Potential contours. b) Total ion density contours (contour level:  $n_{ion}/n_{bi0} = 10^{-4}, 5 \times 10^{-4}, 10^{-3}, 5 \times 10^{-3}, 10^{-2}, 5 \times 10^{-2}, 0.1, 0.5, 1., 1.5$ ). c) Charge-exchange ion current vectors  $J_{cex}$ .



**Figure 3: Plume ion velocity distributions (left column) and solar wind proton velocity distributions (right column) for the  $\alpha = 0^\circ$  case. The distributions are plotted at  $\Omega_X t = 0$  (solid), 8 (dashed), 16 (dotted), 24 (dot-dashed), and 48 (dot-dot-dashed).**



**Figure 4: Time histories for the  $\alpha = 0^\circ$  case. a) magnetic field fluctuation energy density  $\delta B^2/B_0^2$ . b) plume ion energy densities  $\frac{v_j^2}{2v_{AX}^2}$  ( $j = x$ : solid line;  $j = y$ : dashed line;  $j = z$ : dotted line.)**

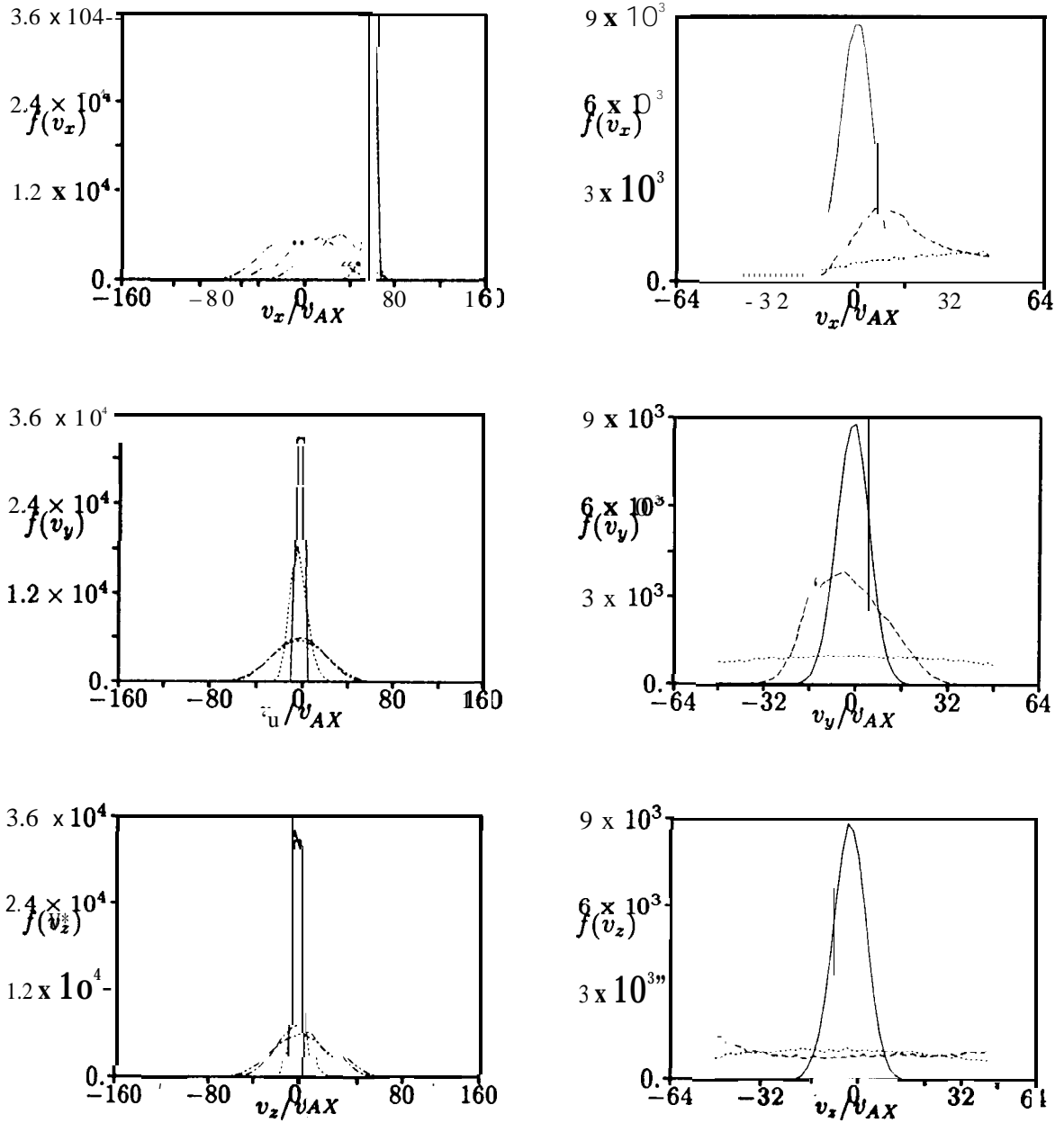


Figure 5: Plume ion velocity distributions (left column) and solar wind proton velocity distributions (right column) for the  $\alpha = 90^\circ$  case. The distributions are plotted at  $\Omega_X t = 0$  (solid), 8 (dashed), 16 (dotted), 24 (dot-dashed), and 48 (dot-dot-dashed).

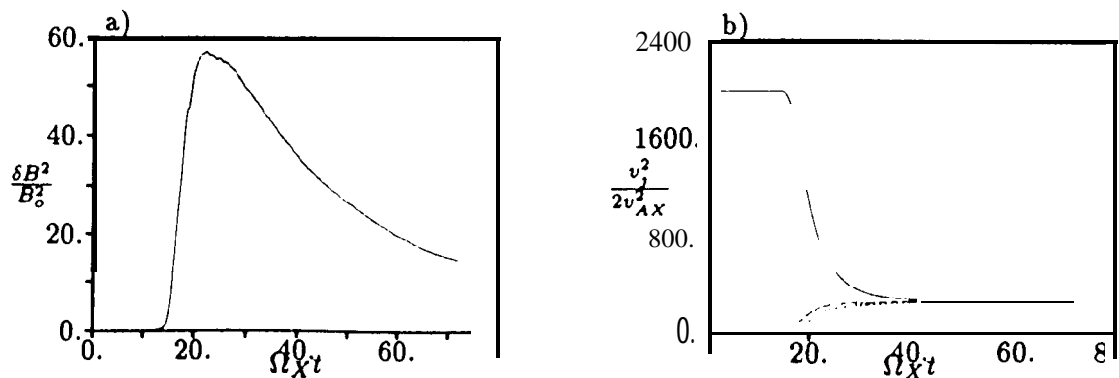


Figure 6: Time histories for the  $\alpha = 90^\circ$  case. a) magnetic field fluctuation energy density  $\delta B^2 / B_0^2$ . b) plume ion energy densities  $\frac{v_j^2}{2v_{AX}^2}$ . ( $j = x$ : solid line;  $j = y$ : dashed line;  $j = z$ : dotted line.)